

Research Article

Design of Phase Shifters with Enhanced Selectivity and Miniaturized Size Using D-CRLH Resonator

Zhe Chen,^{1,2} Jingbo Wang ,¹ and Jianxun Tang¹

¹School of Information and Communication, Guilin University of Electronic Technology, Guilin 541004, China

²Cognitive Radio and Information Processing Key Laboratory Authorized by China's Ministry of Education Foundation, Guilin University of Electronic Technology, Guilin 541004, China

Correspondence should be addressed to Jingbo Wang; bossge@mails.guet.edu.cn

Received 29 June 2023; Revised 18 September 2023; Accepted 2 December 2023; Published 18 December 2023

Academic Editor: Chien-Jen Wang

Copyright © 2023 Zhe Chen et al. This is an open access article distributed under the Creative Commons Attribution License, which permits unrestricted use, distribution, and reproduction in any medium, provided the original work is properly cited.

This paper proposes and demonstrates a novel filtering phase shifter with a compact size and good frequency selectivity using two dual composite right/left-handed (D-CRLH) resonators. Firstly, the study analyzes the D-CRLH structure to gain insights into its unique properties, providing a physical understanding for subsequent design procedures. Then, an ad hoc systematic design procedure for the D-CRLH phase shifter is discussed in detail. Different from the traditional phase shifter, the innovative integration of D-CRLH structure in phase shifters enables its advantages in the flexible realization of good in-band frequency selectivity and compact size. This advantageous utilization of the D-CRLH structure distinguishes our proposed phase shifter from conventional implementations. Finally, to demonstrate the feasibility of the proposed structure, we design, fabricate, and measure a prototype of the filtering phase shifter with a 90° phase shift. The comparison between simulation and measurement results shows good agreement, thereby confirming the effectiveness of both the new filtering phase shifter and the presented design procedure. Through this comprehensive investigation, our work showcases a promising solution for achieving compact size, good frequency selectivity, and reliable performance in phase shifter design.

1. Introduction

Due to the rapid development of modern wireless communication systems, particularly the emergence of the fifth-generation (5G) communication technology, there is an increasing demand for microwave components with small size, high integration, and excellent performance. To meet this growing demand, a crucial strategy is to design a class of multi-function filtering phase shifters with both filtering and phase-shifting functions. These components are widely used in beamforming networks and phased array antenna systems [1–3], making their design critically important. As a result, the high-performance phase shifters have gained significant attention over the last few decades, with many designs being reported [4, 5]. The Schiffman phase shifter [6] has emerged as one of the most classical phase shifters and has been a popular research topic since its inception.

In [7–10], several types of Schiffman phase shifters are introduced. However, due to the increasingly complex communication situation, this classical phase shifter suffers from the disadvantage of poor frequency selectivity, rendering it inadequate for meeting the practical performance requirements. As an alternative method to overcome this disadvantage, a filtering phase shifter is proposed, which involves the codesign of a phase shifter and a filter as a single component. This approach utilizes coupled substrate integrated waveguide (SIW) resonators, although it introduces complexities in the manufacturing process and results in higher insertion loss [11]. More recently, inspired by a similar concept presented in [12–14], another method has emerged that employs microstrip line (MSL) resonators for implementing a new topology of filtering phase shifters in antenna feeding networks. The authors of [15–23] have presented us with some phase shifter structures in recent

years, greatly broadening our horizons and expanding our knowledge in this field.

However, many previously reported works employ $\lambda/2$ or $\lambda/4$ transmission line resonators as building blocks, which result in a large physical size that is impractical for RF applications. To address this limitation, a recent approach presented in [24] introduces a dual-band 90° phase shifter that leverages the advantageous properties of via-free D-CRLH resonators to achieve miniaturization. Nonetheless, this design suffers from a high sensitivity to frequency variation, and it only maintains a constant phase shift near the center frequency. To overcome the aforementioned challenges encountered in prior studies, this paper proposes a novel phase shifter that offers good frequency selectivity and compact size by utilizing D-CRLH resonators. This innovative design aims to mitigate the drawbacks identified in previous approaches.

2. Proposed Wideband Phase Shifter Structure

In Figure 1(a), the D-CRLH resonator is researched and developed, which consists of a high impedance line (l_1, w_2), parallel coupling lines (l_2, w_1, s_1), and 50Ω feed lines as ports. The required performance can be achieved through the size tuning of the resonator, which provides great design flexibility.

Figure 1(b) presents the LC equivalent circuit of a π -type D-CRLH resonator structure [25] which is composed of a series of the parallel resonant circuit and two parallel series resonant circuits. In the paper, we establish an accurate equivalent circuit model and introduce a D-CRLH unit cell for assisting in the design. C_1 represents the capacitance of the interdigital capacitor, L_1 represents the inductance of the shunt metal wire, $C_2/2$ represents the coupling between the resonator and the ground, and $2L_2$ represents the leakage effect excited by the resonator to the ground. Based on the admittance matrix of D-CRLH unit, the equivalent circuit with L_1, L_2, C_1 , and C_2 elements can be obtained by calculation. This structure will produce two kinds of resonance, corresponding to the right hand in the low-frequency band and the left hand in the low-frequency band, and the left hand in the high-frequency band [26] gives the derivation process in detail about the relevant components in the equivalent circuit. Therefore, these parameters can be determined by formulas (1)–(5):

$$K_g = 0.57 - 0.145 \ln\left(\frac{w_2}{h}\right), \frac{w_2}{h} > 0.05, \quad (1)$$

$$L_1 = 2 \times 10^{-4} l_1 \left[\ln\left(\frac{l_1}{w_2 + t}\right) + 1.193 + \frac{w_2 + t}{3l_1} \right] \times K_g, \quad (2)$$

$$L_2 = 2\tau L_1, \quad (3)$$

$$C_1 = 0.559 \times 10^{-5} l_1 (\epsilon_r + 1), \quad (4)$$

$$C_2 = \frac{\epsilon_r \epsilon_0 S_{\text{metal}}}{2h}, \quad (5)$$

where ϵ_r is the dielectric constant of the substrate, S_{metal} is the metal area of the D-CRLH resonator, h is the thickness of the substrate, t is the thickness of the printed metallic layer, and τ is the correlation index.

Through the above theoretical formula analysis, we give an example for verification. According to the theoretical formula in [27] and (1)–(5), we get accurate calculation results. Based on the above analysis and the equivalent circuit model in Figure 1(b), the resonant frequency band of RH and LH resonators f_{RH} and f_{LH} can be calculated by the following formula:

$$\begin{aligned} f_{\text{RH}} &= \frac{1}{(2\pi\sqrt{L_1 C_1})}, \\ f_{\text{LH}} &= \frac{1}{(2\pi\sqrt{L_2 C_2})}. \end{aligned} \quad (6)$$

The frequency response of the equivalent circuit and topology is shown in Figure 1(c), where, specifically, the right-hand response is near 1.6 GHz, the left-hand response is near 6 GHz, and the spurious response is near 5 GHz. The design of this paper is only in the lower right-hand frequency band.

3. Design of D-CRLH Phase Shifter

3.1. Design of Bandpass Filter. In Figure 2(a), a second-order BPF using the D-CRLH resonator is designed. The coupling gap between the two D-CRLH resonators is s_2 . To achieve the required external coupling, we connect both feed lines with the resonator. In Figure 2(b), we give the equivalent circuit of the proposed filter, where L_{11} represents the uncoupled equivalent inductance of the transmission line, L_{12} represents the coupled equivalent inductance of the transmission line, C_1 and L_{13} represent the equivalent capacitance and inductance of the interdigital capacitor, respectively, and C_q represents the coupling between the port and each single-mode resonator. In addition, the coupling between adjacent resonators is a hybrid electromagnetic coupling, which is further represented by the coupling coefficient M and the capacitance C_m , and then M and C_m are constrained by gap s_2 . For second-order BPF, the characteristics of passband are constrained by the resonators and their external and internal coupling. The center frequency of the BPF is determined by the RH response frequency of the D-CRLH unit cell, and we give the corresponding S-parameters of the designed BPF in Figure 2(c).

3.2. Design of Phase Shifter. In Figure 3, we give the topology of the proposed phase shifter, which is composed of two different D-CRLH BPFs, in which the BPF_r branch is used as the reference line and the BPF_m branch is used as the phase adjustment line. BPF_r and BPF_m are second-order BPFs using the D-CRLH resonator. Compared with the traditional phase shifter, our proposed differential phase shifter provides both constant phase shift and narrowband filtering functions.

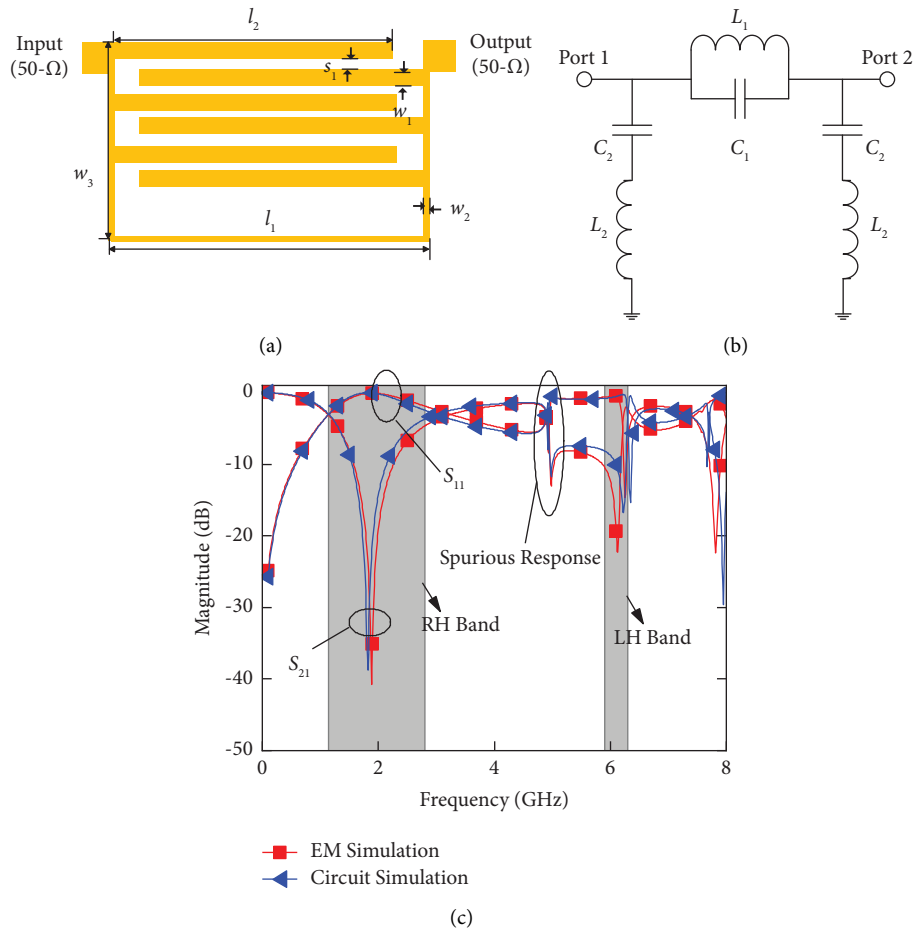


FIGURE 1: (a) D-CRLH unit cell schematic layout. (b) Proposed π -type D-CRLH circuit. (c) Unit cell schematic layout S-parameters.

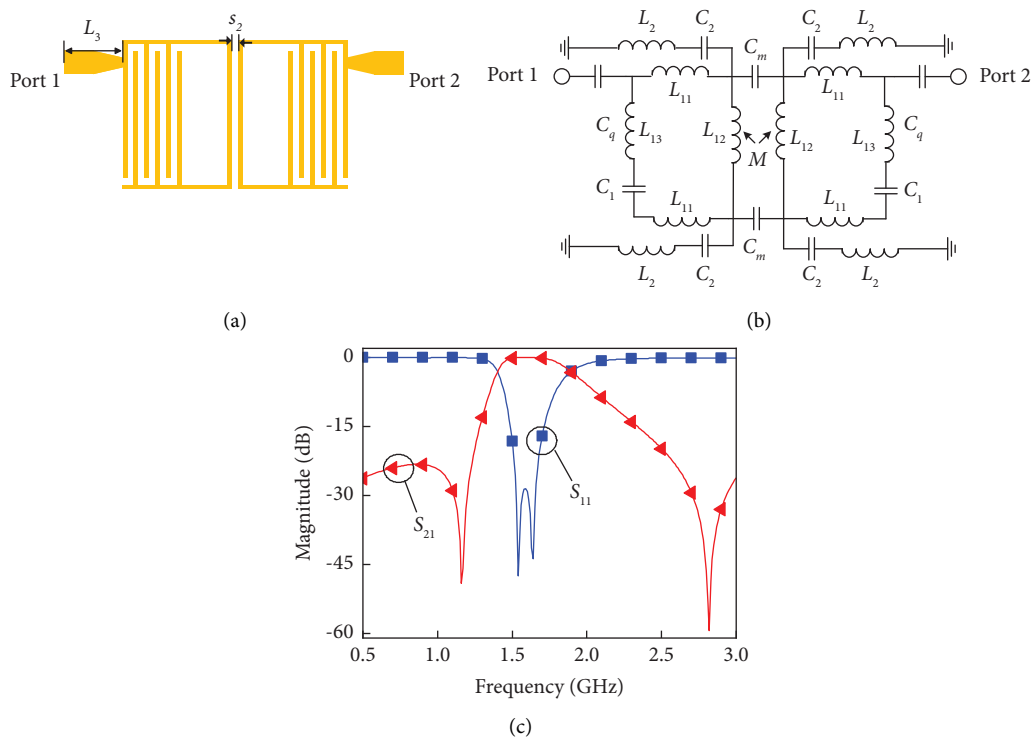


FIGURE 2: (a) Schematic layout of the D-CRLH bandpass filter. (b) Equivalent circuit of the D-CRLH BPF. (c) S-parameters of the D-CRLH BPF.

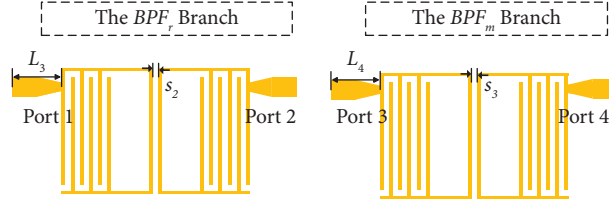


FIGURE 3: Schematic layout of the phase shifter.

As for a bandpass filter, the higher cutoff frequency of the passband is defined as f_H , and its lower cutoff frequency is defined as f_L , from which the calculation formula for center frequency can be obtained:

$$f_0 = \sqrt{f_H \times f_L}. \quad (7)$$

When designing the phase shifter (D-CRLH), we first design the reference branch shown in Figure 3. Based on the designed reference portion, to realize any phase shift, the electrical length $\theta_{\text{delay}0}$ of the delay line can be determined at first according to the phase shift $\Delta\Phi_0$ at center frequency f_0 .

Therefore, we define the phases of branch BPF_m and branch BPF_r as Φ_m and Φ_r , and the calculation formula of phase shift $\Delta\Phi$ can be obtained:

$$\Delta\Phi = \Phi_m - \Phi_r = 2\theta_{\text{delay}}(f_0) = 2\theta_{\text{delay}0}. \quad (8)$$

According to the microwave network theory, in the symmetrical network, we can use an $ABCD$ transmission matrix to calculate the transmission coefficient S_{21} and the insertion phase of BPF.

S_{21} can be represented by the $ABCD$ matrix as

$$S_{21} = \frac{2}{(A + B/Z_0 + CZ_0 + D)}. \quad (9)$$

The insertion phase of BPF is

$$\angle S_{21} = -\tan^{-1} \frac{B + CZ_0^2}{j(A + D)Z_0}. \quad (10)$$

Through the above analysis, we find that the design between the two branches has great flexibility and can be optimized independently. This can not only reduce the design difficulty but also get better phase-shifting performance.

4. Experiment Results and Discussion

In this section, we give the specific design method of the proposed phase shifter to verify the accuracy of our proposed theory. The designed phase shifter is constructed on a single-layer substrate. The design is implemented on the Rogers 5880 structure ($\epsilon_r = 2.2$, $h = 0.787$ mm, and $\tan\delta = 0.0009$). The bandwidth range of phase shifter is 1.51–1.69 GHz, the working center frequency is 1.6 GHz, the fractional bandwidth (FBW) is 11.32%, the minimum return loss (RL) is less than 18.17 dB, and the insertion loss (IL) is more than 0.46 dB. The structural electric size of the proposed phase shifter is $0.297 \lambda_g \times 0.197 \lambda_g$. Overall, these parameters showcase the high performance of our proposed

TABLE 1: Size of the BPF_m branch.

Branch	45° (mm)	90° (mm)	135° (mm)	180° (mm)
s_3	0.11	0.11	0.085	0.10
l_4	20	28.8	39.23	47.56

design and its ability to achieve the desired outcomes with limited IL and greater FBW.

Next, we have designed 45°, 90°, 135°, and 180° phase shifters. Due to the principle of joint design of filter and phase shifter, the four groups of phase shifter reference branches in this design adopt the same structure, and only the main branch is structurally optimized. The structure of the phase shifter is shown in Figure 3, and its practical implementation requires high machining accuracy and low fabrication tolerance. The specific physical sizes of the four groups of main branches are shown in Table 1. By analyzing the simulated results of four groups of phase shifters, their center frequency can reach about 1.59 GHz and the passband range is about 1.51–1.69 GHz, indicating that they have well met our design expectations. In the study of [28, 29], we have also learned that the larger the phase shift value of the phase shifter pair, the narrower the bandwidth of the phase shifter. The S-parameters of the four groups of the main branch are shown in Figure 4(a), their phase shift results are shown in Figure 4(b), and the group delays are shown in Figure 4(c). Within the passband range, the four groups of phase shifters can achieve the phase shift range of $45 \pm 2^\circ$, $90 \pm 5^\circ$, $135 \pm 4^\circ$, and $180 \pm 7^\circ$. This result is also in line with our expected value of phase shift performance of phase shifter.

To verify the performance reliability of the phase shifter we designed, we have fabricated a 90° phase shifter and compared the measured results with the simulation results. Figure 5(a) is the comparison of the reference branch S-parameters of the 90° phase shifter, Figure 5(b) is the comparison of the main branch S-parameters of the 90° phase shifter, and Figure 5(c) is the comparison of the phase shift of the 90° phase shifter around the center frequency. Figure 6 shows the complete design process for proposing a phase shifter. We also compare it with other phase shifter structures in Table 2. Through our analysis, we conclude that the designed phase shifter satisfies the performance requirements of modern communication systems, such as Butler matrix or circularly polarized antenna structures. It excels particularly in demanding working conditions that necessitate high-performance RF components, demonstrating excellent frequency selectivity and precise phase-shifting capabilities.

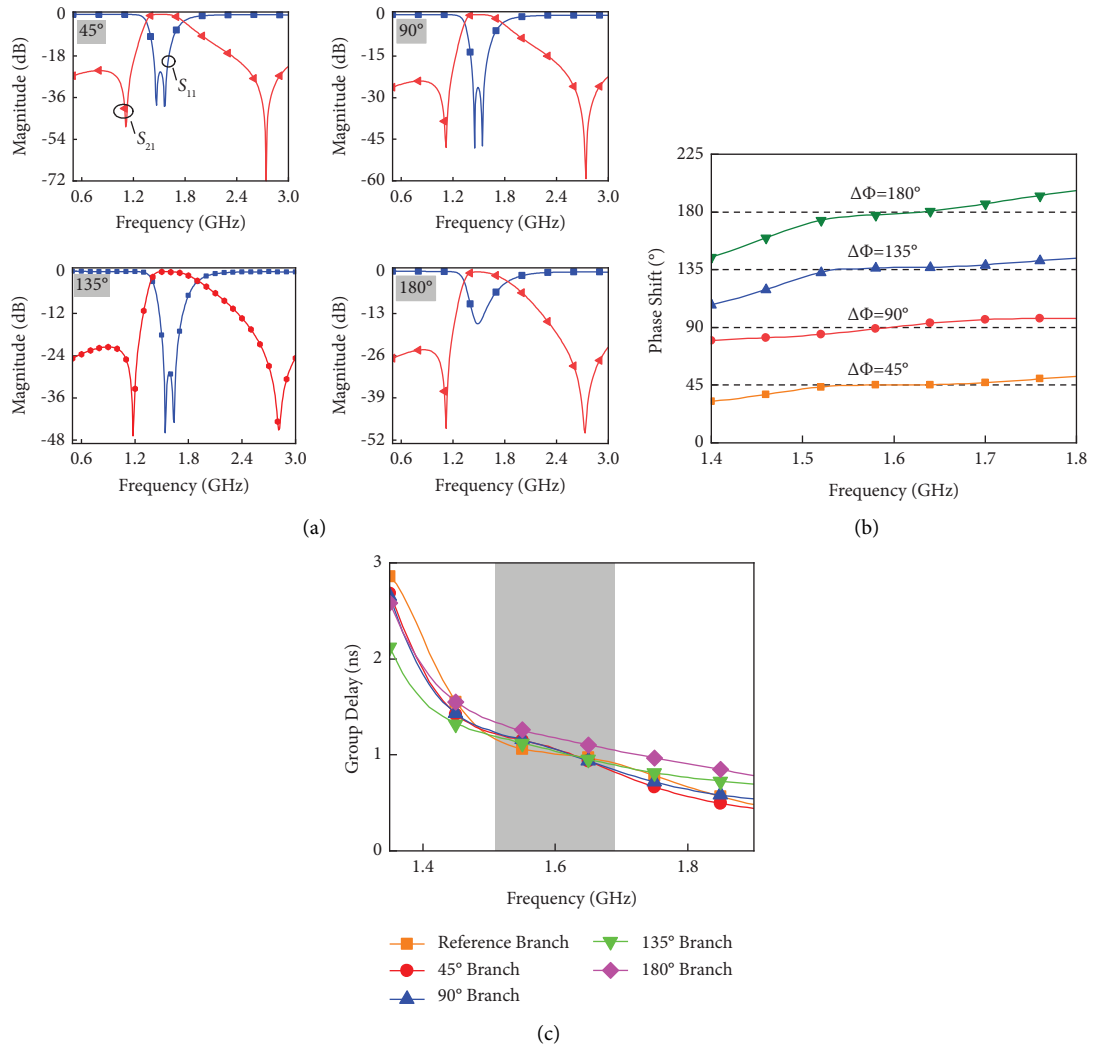


FIGURE 4: (a) S-parameters of the phase shifters. (b) Phase shifts. (c) Group delay of five structures.

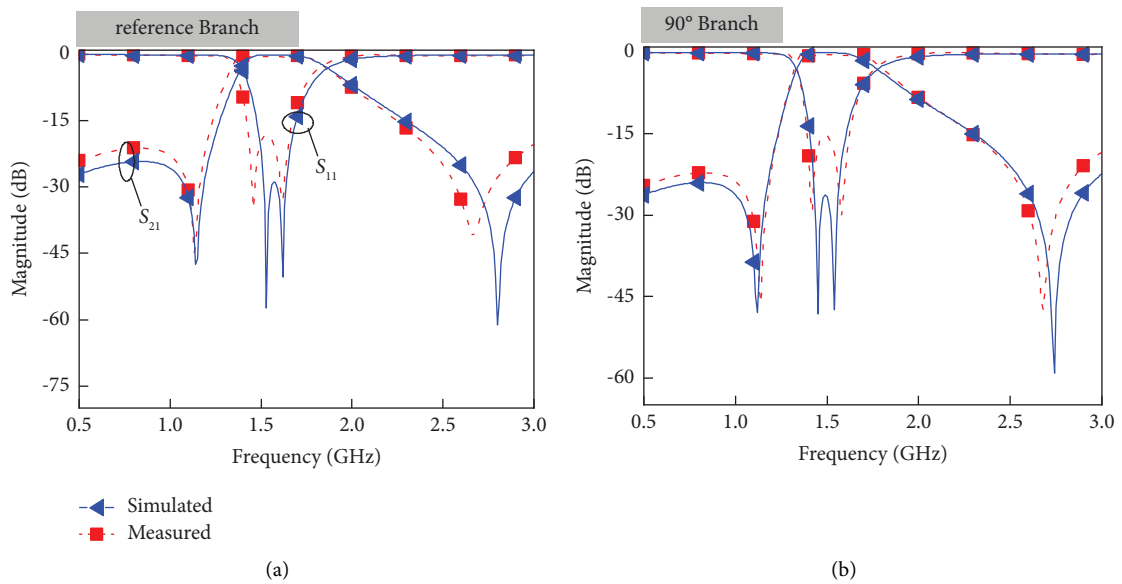


FIGURE 5: Continued.

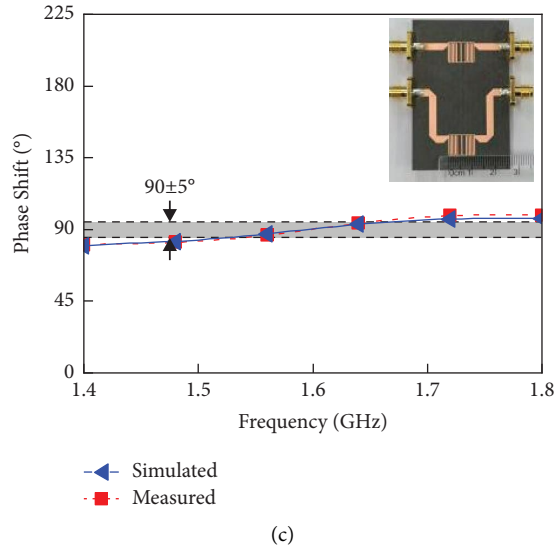


FIGURE 5: Simulated and measured frequency responses of the proposed 90° phase shifter. (a) S-parameters of reference branch. (b) S-parameters of 90° branch. (c) Phase shift response (the inset is its photograph).

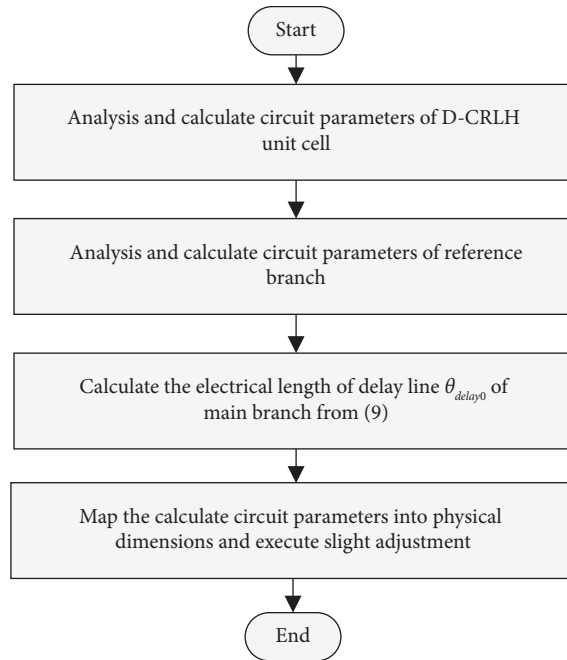


FIGURE 6: Flowchart for design of the proposed D-CRLH phase shifter.

TABLE 2: Performance comparison with different phase shifters.

	f_0 (GHz)	Phase shift \pm PD ($^\circ$)	IL (dB)	RL (dB)	Number of TZs	FBW (%)	Size (λ_g^2)
[6]	10.00	80 ± 5	4	13.00	0	7.40	0.86×0.78
[8]	5.00	$90@f_0$	N.A.	16.50	0	≈ 7.07	$\approx 1.50 \times 1.40$
[9]	4.00	$90@f_0$	N.A.	10.00	0	≈ 8.80	$\approx 1.00 \times 0.90$
[10]	1.62	$91@f_0$	0.17	15.70	1	4.00	0.35×0.33
[15]	2.00	180 ± 2	0.22	10.00	0	15.00	0.70×0.19
[16]	8.50	90 ± 5	0.70	N.A.	0	35.00	0.84×0.80
[17]	26.00	90 ± 5	1.30	15.00	0	39.30	2.18×1.31
This work	1.59	90 ± 5	0.46	18.17	2	11.32	0.297×0.197

5. Conclusions

In this paper, we have conducted a thorough investigation into the characteristics of D-CRLH cells. By adopting a co-design approach involving both the bandpass filter (BPF) and the phase shifter, we have successfully obtained a phase shifter structure that aligns with our desired design expectations. This proposed structure not only exhibits a compact size but also offers a diverse range of adjustable parameters, greatly enhancing the design flexibility. Furthermore, the excellent agreement observed between the simulated and measured results serves as a strong validation of the achieved goals in terms of size miniaturization, frequency selectivity, and the ability to achieve arbitrary phase shift values. Consequently, our study highlights the promising potential of utilizing the D-CRLH filter in various applications in the future. Overall, this work demonstrates the feasibility and effectiveness of our proposed design, paving the way for further advancements and utilization of the D-CRLH filter in diverse practical scenarios.

Data Availability

The data used to support the findings of this study are available from the corresponding author upon reasonable request.

Conflicts of Interest

The authors declare that they have no conflicts of interest.

Acknowledgments

This project was supported by the 2021 Open Fund Project of the Key Laboratory of Cognitive Radio and Information Processing of the Ministry of Education and the Innovation Project of GUET Graduate Education (2022YCXS029 and 2023YCXS021).

References

- [1] X. Zhu, T. Yang, P. L. Chi, and R. Xu, "Novel passive vector-sum reconfigurable filtering phase shifter with continuous phase-control and tunable center frequency," *IEEE Transactions on Microwave Theory and Techniques*, vol. 70, no. 2, pp. 1188–1197, 2022.
- [2] P.-L. Chi, S.-A. Shang, and T. Yang, "Novel compact coupler with tunable frequency, phase difference, and power-dividing ratio," *IEEE Microwave and Wireless Components Letters*, vol. 31, no. 10, pp. 1119–1122, 2021.
- [3] X. Zhu, T. Yang, P. L. Chi, and R. Xu, "A tunable vector-sum filtering power divider with continuously tuned frequency and arbitrary output phase difference," *IEEE Microwave and Wireless Components Letters*, vol. 30, no. 11, pp. 1033–1036, 2020.
- [4] Y. Lin, C.-Y. Hsiao, P.-L. Chi, and C.-N. Kuo, "A 39 GHz reflection-type phase shifter for reflectarray antenna application," in *Proceedings of the VLSI Design, Autom. Test (VLSI-DAT)*, pp. 1–3, Hsinchu, Taiwan, April 2019.
- [5] P.-L. Chi and C.-L. Huang, "Reconfigurable 1.5–2.5-GHz phase shifter with 360° relative phase-shift range and reduced insertion-loss variation," in *Proceedings of the 2017 IEEE MTT-S Int. Microw. Symp.*, pp. 897–899, Honolulu, HI, USA, June 2017.
- [6] B. M. Schiffman, "A new class of broad-band microwave 90-degree phase shifters," *IEEE Transactions on Microwave Theory and Techniques*, vol. 6, no. 2, pp. 232–237, 1958.
- [7] J. L. R. Quirarte and J.-P. Stanski, "Novel Schiffman phase shifters," *IEEE Transactions on Microwave Theory and Techniques*, vol. 41, no. 1, pp. 9–14, 1993.
- [8] Y.-X. Guo, Z.-Y. Zhang, and L.-C. Ong, "Improved wide-band Schiffman phase shifter," *IEEE Transactions on Microwave Theory and Techniques*, vol. 54, no. 3, pp. 1196–1200, 2006.
- [9] Y.-P. Lyu, L. Zhu, Q.-S. Wu, and C.-H. Cheng, "Proposal and synthesis design of wideband phase shifters on multimode resonator," *IEEE Transactions on Microwave Theory and Techniques*, vol. 64, no. 12, pp. 4211–4221, 2016.
- [10] S.-Y. Zheng, W.-S. Chan, and K.-F. Man, "Broadband phase shifter using loaded transmission line," *IEEE Microwave and Wireless Components Letters*, vol. 20, no. 9, pp. 498–500, 2010.
- [11] W. Hu, D. Jiang, W.-Y. Zhang, Y.-X. Liu, K. Zhu, and T. Zhang, "Design of a W-band dielectric phase shifter based on liquid crystal," *International Journal of Antennas and Propagation*, vol. 2022, Article ID 6486628, 6 pages, 2022.
- [12] Y. Lyu, L. Zhu, and C. Cheng, "Proposal and synthesis design of differential phase shifters with filtering function," *IEEE Transactions on Microwave Theory and Techniques*, vol. 65, no. 8, pp. 2906–2917, 2017.
- [13] Q. Wu, X. Zhang, and L. Zhu, "A feeding technique for wideband CP patch antenna based on 90° phase difference between tapped line and parallel coupled line," *IEEE Antennas and Wireless Propagation Letters*, vol. 18, no. 7, pp. 1468–1471, 2019.
- [14] Q. Wu, X. Zhang, and L. Zhu, "Co-design of a wideband circularly polarized filtering patch antenna with three minima in axial ratio response," *IEEE Transactions on Antennas and Propagation*, vol. 66, no. 10, pp. 5022–5030, 2018.
- [15] F. Liu, J. Xu, Y.-W. Duan, H. Wan, H. Zhang, and L. Zhu, "A 5-bit digital phase shifter using phase-tuning property of open-/short-circuit microstrip line-loaded slot line structure," *IEEE Transactions on Microwave Theory and Techniques*, vol. 71, no. 6, pp. 2606–2615, 2023.
- [16] S. Liu and F. Xu, "Novel substrate-integrated waveguide phase shifter and its application to six-port junction," *IEEE Transactions on Microwave Theory and Techniques*, vol. 67, no. 10, pp. 4167–4174, 2019.
- [17] W. Zhang, Z. Shen, K. Xu, and J. Shi, "A compact wideband phase shifter using slotted substrate integrated waveguide," *IEEE Microwave and Wireless Components Letters*, vol. 29, no. 12, pp. 767–770, 2019.
- [18] A. Singh and M. K. Mandal, "Electronically tunable reflection type phase shifters," *IEEE Transactions on Circuits and Systems II: Express Briefs*, vol. 67, no. 3, pp. 425–429, 2020.
- [19] Y. Shang, Q.-S. Zeng, W.-Z. Gui, X.-W. Wang, and G.-Q. Zheng, "Design of pattern reconfigurable patch antenna array based on reflective phase-shifter," *International Journal of Antennas and Propagation*, vol. 2022, Article ID 2803285, 10 pages, 2022.
- [20] C.-T. Miasaki, E.-M.-C. Franco, and R.-A. Romero, "Transmission network expansion planning considering phase-shifter transformers," *International Journal of Antennas and Propagation*, vol. 2012, Article ID 527258, 10 pages, 2012.
- [21] L. Guo, H. Zhu, and A. Abbosh, "Wideband phase shifter with wide phase range using parallel coupled lines and L-shaped networks," *IEEE Microwave and Wireless Components Letters*, vol. 26, no. 8, pp. 592–594, 2016.

- [22] X. Sun, J.-M. Fernández-González, M. Sierra-Pérez, and B. Galocha-Iragüen, "Low-loss loaded line phase shifter for radar application in x band," in *Proceedings of the 2018 48th European Microwave Conference (EuMC)*, pp. 1497–1500, Madrid, Spain, September 2018.
- [23] Y. Yuan, S. Jammy Chen, and C. Fumeaux, "Varactor-based 360° differential phase shifter pair," in *Proceedings of the 2023 5th Australian Microwave Symposium (AMS)*, pp. 29–30, Melbourne, Australia, February 2023.
- [24] T. Huang, L. Feng, L. Geng et al., "Compact dual-band Wilkinson power divider design using via-free D-CRLH resonators for beidou navigation satellite system," *IEEE Transactions on Circuits and Systems II: Express Briefs*, vol. 69, no. 1, pp. 65–69, 2022.
- [25] G. Shen, W. Che, W. Feng, and Q. Xue, "Analytical design of compact dual-band filters using dual composite right-/left-handed resonators," *IEEE Transactions on Microwave Theory and Techniques*, vol. 65, no. 3, pp. 804–814, 2017.
- [26] T. Yang, M. Tamura, and T. Itoh, "Compact hybrid resonator with series and shunt resonances used in miniaturized filters and balun filters," *IEEE Transactions on Microwave Theory and Techniques*, vol. 58, no. 2, pp. 390–402, 2010.
- [27] I. Bahl, *Lumped Elements for RF and Microwave Circuits*, Artech House, Norwood, MA, USA, 2003.
- [28] L.-P. Feng, J. Chen, X.-H. Yu, L. Zhu, and H.-W. Liu, "A novel wideband 90° filtering phase shifter using broadside-coupled MSLs," *IEEE Transactions on Circuits and Systems II: Express Briefs*, vol. 69, 2022.
- [29] X.-H. Yu, J. Chen, L.-P. Feng, L. Zhu, and H.-W. Liu, "Synthesis design of wideband phase shifters using coupled-line structure," *IEEE Microwave and Wireless Components Letters*, vol. 32, no. 6, pp. 515–518, 2022.